26th EPS Conf. on Contr. Fusion and Plasma Physics, Maastricht, 14 - 18 June 1999 ECA Vol.23J (1999) 1653 - 1656

An Electromagnetic Particle-in-Cell Model for a Lower Hybrid Launcher

K.M. Rantamäki[1], K.M. Alm[2], T.J.H. Pättikangas[1], S.J. Karttunen[1],
J.P. Verboncoeur[3], P. Mardahl[3]
[1]*Association Euratom–Tekes, VTT Energy, P.O. Box 1604, FIN-02044 VTT, Finland*
[2]*Association Euratom–Tekes, Helsinki University of Technology, Advanced Energy Systems, P.O. Box 2200, FIN-02015 HUT, Finland*
[3]*Electronics Research Laboratory, University of California, Berkeley, CA 94720, USA*

I. INTRODUCTION

In lower hybrid (LH) current drive, an efficient coupling of the wave power to tokamak plasmas is one of the key issues. The coupling is usually modelled with the aid of the linear wave equation [1,2] by neglecting kinetic and non-linear effects in the near-field of the launcher. In some cases, however, the kinetic effects are important because the absorption of the LH power in the edge plasma generates hot electrons [3]. In addition, non-linear processes, such as parametric instabilities, are known to occur in front of the LH launcher [4]. Self-consistent particle-in-cell (PIC) simulations of the near-field of the launcher offer a tool to study the coupling problem including both kinetic and non-linear effects [5].

In this work, the two-dimensional electromagnetic particle-in-cell code OOPIC [6] has been used for modelling the LH launcher. OOPIC (Object Oriented Particle-in-Cell) allows simulations in fairly complicated geometries with various boundary conditions. The simulations demonstrate the possibilities of electromagnetic PIC simulations in modelling the coupling of the wave power to the plasma.

II. SIMULATION MODEL

In this work, the Object-Oriented Particle-in-Cell code OOPIC [6] is used. The object-oriented implementation helps to maintain and extend the code. The code is two-dimensional in configuration space and three-dimensional in velocity space. The electric and magnetic fields have also all the three components. The particle motion and the EM-fields are treated self-consistently.

The geometry of the OOPIC simulations may be chosen between a cylindrical (zr) or a Cartesian (xy) one. The charge and current densities as well as the fields are calculated on an orthogonal, potentially non-uniform mesh. The field solver is either electromagnetic or electrostatic and the particles may be treated either relativistic or non-relativistic.

A variety of boundary conditions of even complicated shapes can be used in OOPIC, e.g., boundaries for perfect conductors and dielectrics. Some of the boundaries can be used to emit or absorb waves. For particles the boundaries are usually absorbing. However, one can model incoming particle beams with OOPIC. There is also a possibility to emit secondary particles. The code can sustain multiple species and has a package for Monte-Carlo collisions.

In the present paper, a simple 2-dimensional model for the LH grill has been developed to study the coupling problem with OOPIC. The grill consists of 32 parallel plate

waveguides having a width of 8.5 mm, corresponding to the dimensions of the Tore Supra launcher [7]. The waveguides are separated by 2-mm thick perfectly conducting walls. The radial length of the waveguides in this simulation has been chosen to be two vacuum wavelengths, i.e., $L = 16.05$ cm. In the poloidal direction, the waveguides are assumed to be infinitely high. The geometry of the grill mouth is shown in figure 1.

Each waveguide is fed with a pure TEM mode having a frequency of 3.7 GHz. The phase difference between the waveguides is $\pi/2$. The wave launching started at time $t = 1.2$ ns.

The plasma in front of the grill was assumed to have a linear density profile with an edge density of $n_e = 10^{18}$ m^{-3} and a density scale length of $\Lambda_n = 1$ cm. The temperature was assumed to be 25 eV.

The boundaries in the toroidal direction have been chosen to be periodic for the particles. For the wave, these boundaries are absorbing. The high density edge at $x \approx 4$ cm is absorbing both the particles and the wave.

III. SIMULATION RESULTS

Figure 1 shows a contour plot of the toroidal electric field at time $t = 3$ ns. Only the plasma region and plasma facing of the waveguides are shown. The propagation cones of the wave bending towards the upper left corner can be seen. The main contribution comes from the principal mode with a parallel refractive index of $n_{||} \approx 1.9$. However, a weak contribution of the second mode at $n_{||} \approx -5.8$ can also be seen.

At the grill mouth, TM modes are needed to match the TEM fields of the waveguides to the sinusoidal field in the plasma. The TM modes are evanescent and cannot propagate in the waveguides. The decay length of the nth mode is obtained as $L_n = 1/\gamma_n$ [1], where γ_n is defined as

$$\gamma_n = \left[\left(\frac{n\pi}{L_{wg}} \right)^2 - \left(\frac{\omega}{c} \right)^2 \right]^{1/2} . \qquad (1)$$

Here L_{wg} is the width of the waveguide, $\omega = 2\pi f$ is the frequency of the wave and c is the speed of light. For the lowest order evanescent TM modes the decay lengths are $L_1 = 0.28$ cm, $L_2 = 0.14$ cm and $L_3 = 0.09$ cm.

In figure 2, the toroidal electric field versus the toroidal co-ordinate z is shown at two different distances from the grill mouth at time $t = 9$ ns. Inside the grill, near the mouth, one can see the field peaked at the walls. However, the peaks vanish inside the waveguides as the evanescent TM modes die out. Ten decay lengths away the TM modes have disappeared and the field looks like the TEM mode.

The radial field component (not shown) behaves in similar manner. At the grill mouth, the field is peaked at the walls of the waveguides. Due to the evanescence of the TM modes the peaks again vanish when moving towards the wave source. Far away from the grill mouth, the peaks are no longer seen and the radial field component tends to zero.

The power spectrum is shown in figure 3 at three locations at the time $t = 9$ ns. Figure 3(c) shows the spectrum inside the waveguides. One can see that most of the power is in the principal mode $n_{||} \approx 1.9$. However, there is also some power in the mode at $|n_{||}| \approx 5.8$. The power spectrum changes at the grill mouth, as is seen in figure 3(b). In addition to the peaks mentioned above, the spectrum has peaks between these and with

values higher than $|n_{||}| = 5.8$. The spectrum is still evolving when the wave propagates further into the plasma, as is seen in figure 3(a), which shows the spectrum 2 cm from the grill.

Part of the LH power is reflected back at the grill mouth. This reflection was estimated from the Poynting fluxes. The time histories of the electric and magnetic fields were measured in the waveguides at $x \approx -14.5$ cm. The radial Poynting flux averaged over 4 wave periods was calculated. Figure 4 shows the Poynting fluxes for two typical waveguides.

The reflection coefficient in each waveguide can be determined from the time-averaged Poynting fluxes. The reflection coefficients were first benchmarked against data published by Knowlton and Porkolab [8]. In those cases only four waveguides were used. The results of the simulations were in good agreement with the linear theory.

The simulations were then extended to 32 waveguides. Figure 4(a) shows an example of a waveguide with fairly large reflection, where the decrement of the Poynting flux caused by the reflected wave can be seen clearly. Figure 4(b) shows an example of a waveguide with low reflection. The average reflection coefficient of the grill can be determined from the reflection coefficients of the individual waveguides. In this case, the result was 3.4 %.

IV. SUMMARY

A new promising method for modelling a lower hybrid launcher has been described. A 2d3v electromagnetic particle-in-cell code OOPIC (Object Oriented Particle-in-Cell) was used to investigate the edge plasma. OOPIC enables realistic modelling of the non-linear and kinetic phenomena.

In this study, a 32-waveguide launcher was considered. It was shown that OOPIC is an appropriate tool for modelling the LH grill. The electric field and the field spectra in the near-field of the launcher were analysed. The code described well the launched TEM mode and the reflected TEM and TM modes. The wave power was well coupled to the plasma and the lowest order evanescent TM mode was seen.

[1] M. Brambilla, *Nucl. Fusion* **16** (1976) 47.
[2] D. Moreau, *et al.*, *Radiation in Plasmas*, vol. 1 (World Scientific, Singapore, 1984) 331.
[3] V. Fuchs, M. Goniche, *et al.*, *Phys. Plasmas* **3** (1996) 4023.
[4] M. Brambilla, *Kinetic Theory of Plasma Waves*, (Oxford University Press, 1998).
[5] K.M. Rantamäki, T.J.H. Pättikangas, *et al.*, *Phys. Plasmas* **5** (1998) 2553.
[6] J.P. Verboncoeur, A.B. Langdon, *et al.*, *Comput. Phys. Commun.* **87** (1995) 199.
[7] X. Litaudon, G. Berger-By, *et al.*, *Nucl. Fusion* **32** (1992) 1883.
[8] A. C. England, O. C. Eldridge, *et al.*, *Nucl. Fusion* **29** (1989) 1527.

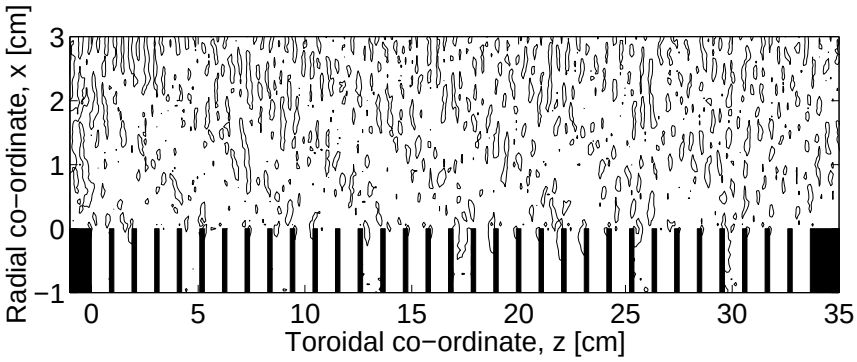

FIG. 1. Contour plot of the toroidal electric fields, E_z. The waveguides are located in the bottom part of the figure.

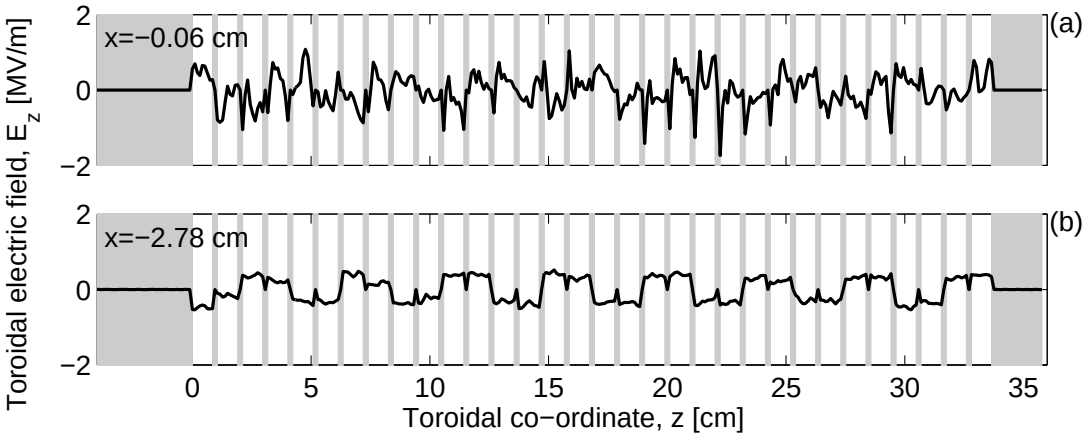

FIG. 2. The toroidal electric fields, E_z versus the toroidal co-ordinate z in the waveguides at different distances from the grill mouth: (a) just inside the grill mouth at $x = -0.6$ mm and (b) ten decay lengths away from the grill mouth at $x = -2.78$ cm. The shaded regions denote the positions of the walls between the waveguides.

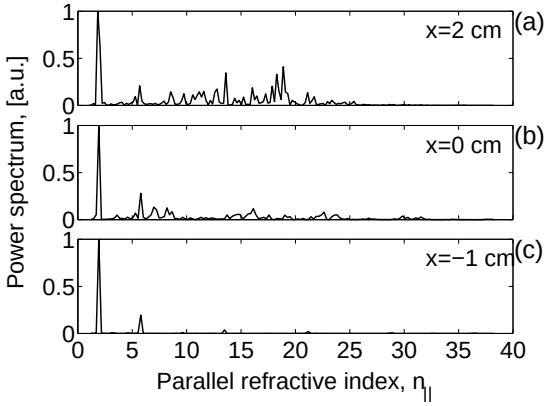

FIG. 3. Power spectra versus the parallel refractive index at different distances from the grill mouth: (a) in the plasma at $x = 2$ cm, (b) at the grill mouth ($x = 0$) and (c) inside the waveguides at $x = -1$ cm.

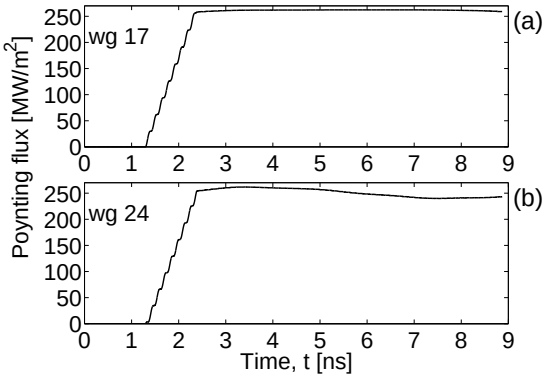

FIG. 4. Time-averaged Poynting flux versus time in two typical waveguides for the grill with 32 waveguides: (a) waveguide #17 (b) waveguide #24.